Polymer 41 (2000) 7705–7713

polymer

Film blowing of linear low-density polyethylene blended with a novel hyperbranched polymer processing aid

Y. Hong[a], S.J. Coombs[a], J.J. Cooper-White[a], M.E. Mackay[a,b,*], C.J. Hawker[c], E. Malmström[d], N. Rehnberg[e]

[a]*Materials Characterization and Processing Centre, Department of Chemical Engineering, The Univerity of Queensland, Brisbane, Queensland 4072, Australia*
[b]*Department of Chemical, Biochemical and Materials Engineering, Stevens Institute of Technology, Castle Point on the Hudson, Hoboken, NJ 07030, USA*
[c]*IBM Almaden Research Laboratories, San Jose, CA, USA*
[d]*Department of Polymer Technology, Royal Institute of Technology, S-100 44 Stockholm, Sweden*
[e]*Perstorp AB, Perstorp, Sweden*

Received 16 September 1999; received in revised form 11 January 2000; accepted 25 January 2000

Abstract

The use of hyperbranched polymer (HBP) as a processing aid for linear low-density polyethylene (LLDPE) in the tubular film blowing process was investigated. Through the addition of HBP, sharkskin was successfully eliminated without significantly changing the overall physical properties of LLDPE films. Also, there was a minimum of 40% enhancement in processing rate with addition of 0.5 wt% HBP. The study showed that HBP and LLDPE are immiscible, and HBP has a tendency to migrate to the surface, subsequently, it seems to form a lubricating layer between the metal surfaces and the bulk material. This phase separation between HBP and LLDPE results in an HBP-rich surface, which has a high potential to create unique surface properties tailored to various applications. Rheological analysis indicated that excessive slip was present in HBP/LLDPE suggesting that the onset of slip is not the cause of sharkskin. On the contrary, it may be partially responsible for the elimination of sharkskin. © 2000 Elsevier Science Ltd. All rights reserved.

Keywords: Processing aids; Hyperbranched polymers; Dendrimers

---

1. Introduction

The use of plastic film has had tremendous growth during the past four decades with a wide range of industrial applications. Low-density polyethylene (LDPE) is a thermoplastic resin mostly used in the manufacture of film by tubular film blowing. LDPE was first produced in 1933 by Imperial Chemical Industries Limited [1], and today, it is the largest sales volume thermoplastic produced in the US with a total production of 13.5×10^9 kg in 1997. LDPE films are used in the packaging industry because they have a good balance of properties such as tensile strength, tear strength, burst strength, impact resistance and sealability. Linear low-density polyethylene (LLDPE) is often used in the stretch wrapping market as it has a greater tear and puncture resistance, and higher tensile strength and higher elongation to break compared to LDPE. Note, the profit margin is so small in the polyethylene processing industry that a slight increase in the production rate, i.e. increased processibility, can offer a significant advantage to manufacturers and bring tremendous cost savings to the processing industry.

The processibility of film is often limited by the occurrence of extrudate irregularities in film blowing operations. The irregularities are usually classified into two groups, surface melt fracture and gross melt fracture. The former occurs under steady flow conditions and it ranges in detail from loss of specular gloss to the more severe form of “sharkskin”. The latter often occurs under unsteady flow conditions and it ranges in appearance from regular (e.g. alternating rough and smooth, or helical) to random distortions [2].

A number of chemicals have been used as processing aids in an attempt to minimize surface irregularities. Blending liquid crystalline polymers (LCPs) with commercial thermoplastics has attracted a great deal of attention over the last decade [3,4]. Although LCPs had the effect of reducing melt viscosity and improving the processibility of PE [4–7], there are a few reasons that limit its application. Firstly, it

---

[*] Corresponding author. Tel.: + 1-201-216-8212; fax: + 1-201-216-8938.

E-mail address: mmackay@stevens-tech.edu (M.E. Mackay).

PII: S0032-3861(00)00130-0

was claimed that LCPs have poor compatibility and interphase adhesion with PE. Also, the processing temperature of common aromatic LCPs is in the range of 300°C, which is much higher than those used for PE processing. Therefore, there is a considerable increase in the energy consumption required and the possibility of PE thermal degradation [3]. The use of an organosilicon chemical (UCARSIL PA-1) as a processing aid was also studied [8–10]. At trace concentration levels, between 500 and 1000 ppm, it was suggested that it aided the extrusion of PE, reduced the extrusion head pressure and extruder torque and eliminated the surface imperfections. A similar effect on processing LLDPE into blown film was also observed [9]. However, no further detailed studies on this matter have been reported.

Fluoroelastomers, such as Viton®, are copolymers of vinylidene fluoride and hexafluoropropylene. They have also attracted extensive industrial attention as processing aids [11–18]. The presence of fluoroelastomers, either as an adhesion promoter [2] or as a slip promoter [15], causes a decrease of the critical shear stress for the onset of slip, consequently, improving the surface appearance [19–22]. It was demonstrated that the polymers have the ability to delay the occurrence of the surface melt fracture for polyethylene at very low concentrations (between 500 and 1000 ppm) without changing the physical properties. However, the main drawback of using fluoroelastomers as processing aids is that a preprocessing time of up to 2 h is required to build up a steady-state fluorocarbon coating on the extruder parts [11,14,16,23].

Hyperbranched polymers (HBPs) were first suggested and used as a novel processing aid by Hong et al. [24]. The HBP enhanced the output rate where sharkskin occurred and also lowers the extrusion power. It was also demonstrated that HBPs not only act as a processing aid but also act as a surface modifier. In other words, HBP can improve the surface properties of final products in addition to serving as a processing aid. None of the currently available materials have such bi-functionality. They are also superior to fluoroelastomers in that no preprocessing time is apparently needed to eliminate the sharkskin of LLDPE melts [24], this was also found in the present study.

Highly branched polymers, such as dendrimers and HBPs, have received extraordinary scientific attention in recent years [25–30,63–66]. In spite of the difference between dendritic macromolecules and hyperbranched polymers [31], both of them have a highly branched 'tree-like' three-dimensional structure with all bonds emanating from a central core. They belong to a new class of synthetic polymers, which differ from linear polymers in that they do not have entangled chains and have numerous reactive chain-ends and surface activity. While dendrimers are prepared in a multi-step sequence and have a precise molecular weight, topology and surface reactivity, hyperbranched polymers are prepared in a single step and have an irregular, polydisperse structure. As a consequence they have a less well-defined three-dimensional shape with a dispersity in molecular weight, branching density and number of end groups.

The generation number of dendrimers is related to the degree of polymerization. A generation is defined as addition of multifunctional monomer units to each end group of the previous generation. Thus, the number of end groups scales as $[f-1]^g$ where f is the monomer functionality (greater than two for dendrimers, linear polymers have f equal to two) and g is the generation number. As the structure and positioning of the functional groups in HBPs are irregular, they have no precise generations with the 'generation' of HBPs usually termed as pseudo-generation. Nevertheless, the advantages of HBPs are that they can be produced in industrial quantities at low cost while maintaining many of the fascinating properties which are similar to those of dendrimers, e.g. low intrinsic viscosity, high solubility and miscibility and high reactivity. Due to their unique structure, HBP molecules can be constructed to have different properties. For example, a HBP can be designed to have large hydrophobic cavities in its interior and a hydrophilic surface outside, or vice versa. Therefore, this novel class of polymers has great potential for a wide range of application in advanced coating, drug delivery, chemical sensing, surface modification and polymer processing [24–28,32,63–66].

In our previous paper [24], we suggested the use of HBP is beneficial to the processing industry. We demonstrated that the addition of HBP at a trace amount (500–1000 ppm) to LLDPE can reduce the apparent melt viscosity and consequently, successfully eliminate surface defects under normal processing conditions. The required power consumption for processing was also significantly decreased. The study confirmed the conclusion of Kim and Webster [33] that branches in polymers play an important role in changing polymer properties, and highly branched polymers can act as rheological property modification agents. The purpose of the present study is to investigate whether such advantages can be achieved in the film blowing operation. The reason for using the tubular film blowing process is that it is one of the most important operations in the polymer processing industry. The aim of our study, more specifically, is to minimize the surface roughness and to improve processibility of LLDPE film in the tubular film blowing process through the addition of HBP. The surface properties of the resulting HBP/LLDPE film are evaluated and the miscibility of the HBP/LLDPE blend is also investigated.

A slip analysis was also performed in an attempt to shed some light on the mechanism of sharkskin elimination in HBP/LLDPE blends. The cause(s) of melt fracture is (are) still not well understood despite the extensive work that has been done over many decades. Excellent and thorough reviews have been published on this subject [34–40], however, two major and controversial theories exist. One hypothesis contended by Benbow and his co-workers [41,42] and supported by others [2,39,43–46], suggested

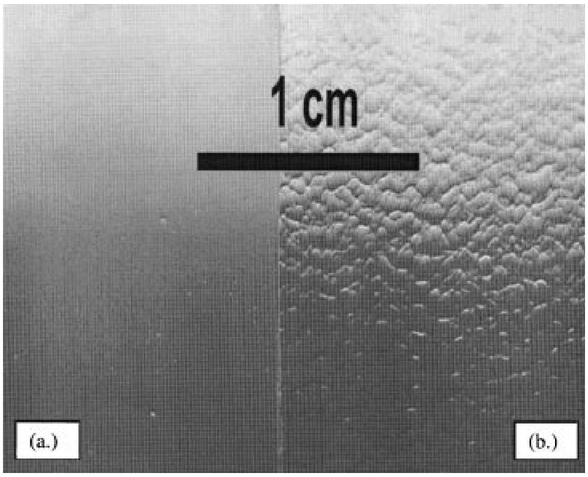

Fig. 1. Surface appearance of the P3GA0.5/LLDPE (left) film and the neat LLDPE (right) film. Note the hyperbranched polymer has reduced the level of surface sharkskin to acceptable levels. Scale bar: 1 cm.

that the onset of slip at the die wall (i.e. failure of adhesion) induces the 'stick-slip' flow, hence developing melt fracture instabilities. On the contrary, some researchers argued that wall slippage, may be a consequence of [47], but not the cause of the sharkskin phenomenon [48,49]. Cogswell [50] and other investigators [42,49,51,52] implied that the die exit singularity, where a velocity and stress discontinuity is found, is responsible for the occurrence of surface defects. Such discontinuities may induce either a high flow stretching rate or a 'cohesive failure' of the polymer melt, consequently, causing the onset of sharkskin [50,52–54]. Corresponding with the speculation by Cogswell, our present study suggests that wall slippage is not the cause of surface defects, on the contrary, it may be one of the factors for surface defect elimination. However, other studies have suggested that explanations based solely on either slip or exit stretching failure are inadequate [52,55]. Further investigation to elucidate the true mechanism of melt fracture elimination is still needed in our opinion.

2. Experimental

2.1. Sample preparation

Perstorp Specialty Chemicals (Perstorp AB, Sweden) produced a series of dendritic additives known as Bolton® H30 [24,56] which are hydroxy-functional dendritic polyesters based on 2,2-bis-methylopropionic acid (bis-MPA) and ethoxylated pentaerytrithol (PP50). Bolton® H30 has a stoichiometric ratio equal to a pseudo-third generation dendrimer based on a four-functional core (i.e. 28:1). It was partially functionalized with a mixture of eicosanoic and docosanoic acid, which was synthesized from Safacid 20/22 (Pronova Oleochemicals, Sandefjord) by acid catalysis and azeotropic removal of water. Ninety percent functionalized Bolton® H30 with a molecular mass of 9000 Da was employed in this study (code named as P3GA). LLDPE reactor powder (no additives), with a melt flow index of 1.0, was provided by Orica Pty Ltd (Australia). Its room temperature density was 925 g/l, and the weight average molecular mass was approximately 130,000 Da with a polydispersity of about 2/1. This molecular mass information was determined for a similar LLDPE, but, from a different batch, via high temperature gel permeation chromatography.

The neat LLDPE and the mixture of LLDPE with the addition of 5 wt% P3GA (code named as P3GA5/LLDPE) were each subjected to extrusion, using an Axon BX-25 Gateway extruder. The extruder barrel was 25 mm in diameter and had a length on diameter ratio of 25/1. The compression ratio was 2.5/1 and was configured as a standard polyethylene screw with several flights cut in the mixing zone to facilitate back mixing. A linear series of five capillaries with diameter of 1 mm were placed at the end of the extruder to produce fibers at a screw speed of 30 rpm, the melt temperature was maintained at 170°C. The P3GA5/LLDPE served as a master batch that was diluted of HBP for the film blowing experiments described below.

Ninety percent of the neat LLDPE pelletized fibers and 10% of the master batch were dry mixed thoroughly, and the mixture (containing 0.5% P3GA in LLDPE, code named as P3GA0.5/LLDPE) was subjected to tubular film blowing again at 170°C. In the process, the extruder was fitted with a bottom fed, spiral die which faces upwards. The film die had a diameter of 40 mm and a die gap of 1 mm. The molten polymer was extruded through the die and the molten tube leaving the die was drawn upwards by nip rolls. The tube was inflated with air to form a bubble, and the molten region of the bubble was controlled by a stream of cooling air via an air ring. Extruder speeds of 30, 40 and 50 rpm were employed respectively. The take up ratio was 28.5 and blow up ratio was 4.5 at 50 rpm. The take-up ratio was defined as the nip rolls linear velocity divided by the average velocity in the die gap. The resulting film tube was collected every 30 s for flow rate analysis.

The films were then subjected to processibility comparison, visual examination, and optical evaluation. Surface analysis including film gloss and roughness tests and X-ray photoelectron spectroscopy (XPS) analysis were performed. The mechanical properties of the films were also investigated. The miscibility of the HBP/LLDPE film was studied using thermal analysis. The master batch of the P3GA5/LLDPE fibers were subjected to rheological slip tests (described below) to begin a preliminarily study of the HBPs sharkskin elimination mechanism.

2.2. Processibility test and surface appearance

The length, thickness, and weight of the resulting films were measured. The linear velocity at the nip rollers and film die and the mass flow rates were calculated. Ten

Table 1
Mechanical properties of LLDPE and HBP/LLDPE films using the film blowing process at an extrusion rate of 40 rpm. The mass flow rates for the two films were almost equivalent at 3.48 ± 0.01 kg/h

Sample	Tensile strength (MPa)	Elongation @ break %	2% Secant modulus (MPa)
LLDPE (MD[a])	38.0 ± 2.7	936 ± 13	259 ± 5
P3GA0.5/LLDPE (MD[a])	29.4 ± 4.3	884 ± 50	269 ± 16
LLDPE (CD[b])	35.5 ± 3.4	1040 ± 78	261 ± 22
P3GA0.5/LLDPE (CD[b])	29.7 ± 3.1	925 ± 58	273 ± 15

[a] MD represents machine direction.

[b] CD represents cross direction.

samples of each film (i.e. LLDPE films and P3GA0.5/LLDPE films) were collected, their mass flow rates were calculated, and the average of the data was used. The apparent die shear rate was then calculated. The apparent shear rate equals $6Q/WH^2$, in which Q represents the volumetric flow rate and W and H stand for the width (mean circumference, 122.5 mm) and height (1 mm) of the film die gap, respectively.

The neat LLDPE film and P3GA0.5/LLDPE film were compared visually as shown in Fig. 1. These photographs were taken with a normal 35 mm camera and lighting to highlight the differences between the two films. Both films were also subjected to light transmission tests at 500 nm using a DMS 90 Varian UV/Visable Spectrophotometer.

2.3. Surface analysis

The resulting films were subjected to film gloss analysis using 75° Hunterlab D48-7 gloss meter. The roughness of the films was investigated using a Parker Print-Surf at 5 kgf/km^2. These are standard tests used in the paper industry and give a representative rating of the film gloss and surface roughness although we recognize other tests are available.

The LLDPE and P3GA0.5/LLDPE films were immersed in *n*-hexane to remove silicone contaminates, and it was assumed that the treatment did not affect the analysis as neither the HBP nor LLDPE are soluble in *n*-hexane. The treated samples were then subjected to XPS surface analysis using a Physical Electronics Industries (PHI, Physical Electronics Division, USA) Model 560 XPS/AM/SIMS I multi-technique surface analysis system employing a model 25-270 AR cylindrical mirror analyzer (CMA). XPS data was collected using Mg Ka1,2 (1253.6 eV) X-rays at 400 W, 15 keV. Survey (wide) scans were recorded with an analyzer pass energy of 100 eV and multiplex high-resolution narrow scans over the C-1s and O-1s regions were taken at a pass energy of 25 and 0.1 eV steps. Atomic concentrations were calculated using peak areas from the high resolution scans and experimental atomic sensitivity factors (ASF) determined by Ward and Wood [57].

2.4. Mechanical testing

The tensile properties of the LLDPE film and the P3GA0.5/LLDPE film were analyzed using an Instron 5584 Mechanical Tester with pneumatic grips (Instron Corporation, USA). The LLDPE and P3GA0.5/LLDPE films were cut into rectangular strips as per ASTM standard D882-95a along the machine direction (MD) and the cross direction (CD) of the films. The width and length of the test specimens were 10 and 150 mm, respectively. The initial grip separation was 100 mm, and the testing crosshead speed, i.e. the rate of separation of the two grips, was set at 10 mm/min. The load (*N*) versus engineering strain (%) was recorded. From this the 2% secant modulus was found. Ten samples of each specimen were tested, and the average data were used and compared in Table 1. All the tests were performed at a constant room temperature of 22°C.

2.5. Thermal characterization

Differential Scanning Calorimetry (DSC) was performed on P3GA (i.e. hyperbranched polymer) powder, LLDPE film, and P3GA0.5/LLDPE film using a DSC 2920 instrument (TA Instruments, USA). Ultra high purity helium was used as the purge gas. The films were weighed and placed into an aluminium pan. The sample pan along with a reference pan were put in a standard DSC cell which was then scanned over a set temperature range at a defined heating/cooling rate. The method involved equilibrating the pans to 0°C, heating them up to 220°C, and then cooling down to 0°C at a constant rate of 10°C/min. The cycle was repeated twice for each experiment. The DSC output curves of heat flow as a function of temperature were recorded to investigate the thermal transitions of the samples.

2.6. Rheological assessments

Melt rheological tests were also performed on the 5% P3GA/LLDPE blends. The discs were made using the method described previously [24]. The tests were performed utilizing a RDS II rheometer (Rheometrics, Inc. USA), with a stainless steel 7.9 mm parallel plate geometry. A constant temperature of 170°C was employed. The materials were tested at gaps of 10–30 μm using the experimental methodology, as outlined by Mackay and Henson [58], to assess what effect the addition of the HBP to LLDPE had on the magnitude of the slip velocity. Our group has previously performed similar analyses on many polymer systems, including LLDPE, and hence direct comparison could be achieved. The technique is fairly straightforward although

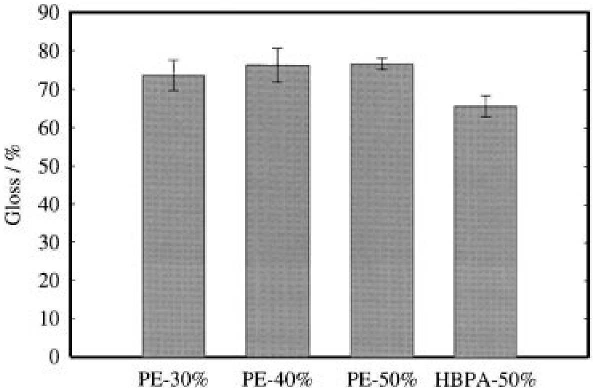

Fig. 2. Comparison of gloss for the neat LLDPE and P3GA0.5/LLDPE blend films manufactured at different extruder speeds expressed as a percentage of full rpm.

it requires great care in alignment and data analysis is tedious. Polished, 7.9 mm diameter, stainless steel plates, to reduce surface roughness, were used and aligned to within 1.3 μm in both concentricity and parallelism [58]. The nominal shear rate including slip effects (γ_N) as a function of radial position (r) in the torsional, parallel plate geometry is

$$\gamma_N(r) = \frac{\Omega r}{H} = \gamma(r) + \frac{2v_s(r)}{H} \tag{1}$$

where Ω is the applied rotational frequency, H the gap between the plates, $\gamma(r)$ the true wall shear rate, which is a function of r, and $v_s(r)$ the slip velocity, which is also a function of r. The factor of '2' is from considering slip at each plate surface. The experiments and analysis must deconvolute the slip velocity from the true wall shear rate and simultaneously determine the true wall shear stress.

The torque (M) balance for the plates is written

$$M = \frac{2\pi R^3}{\gamma_N(R)^3} \int_0^{\gamma_N(R)} \sigma_w(\gamma_N)\gamma_N^2 \, d\gamma_N$$

by using the dummy variable γ_N for r. The maximum radius of the plates is R and $\gamma_N(R)$ is the nominal shear rate at that position. The true shear stress at the wall, σ_w, is written as a function of this variable. Differentiating this equation with respect to $\gamma_N(R)$ results in [59,60]

$$\sigma_w(\gamma_N(R)) = \frac{M}{2\pi R^3}\left[3 + \frac{\partial\, 1n(M)}{\partial\, 1n(\gamma_N(R))}\right] \tag{2}$$

The complete data analysis procedure is:

1. Determine the true wall shear stress as a function of the nominal shear rate via Eq. (2) **at each gap**,
2. Assume a value of $\sigma_w(\gamma_N(R))$ and determine values of $\gamma_N(R)$ at each gap,
3. Plot $\gamma_N(R)$ versus $2/H$ for each assumed $\sigma_w(\gamma_N(R))$, a linear plot should result,
4. The intercept of this plot is the true wall shear rate and the slope is the slip velocity for the assumed wall shear stress according to Eq. (1).

This procedure was performed for the pure LLDPE, however, HBP blend showed unusual results and will be discussed below.

3. Results and discussion

3.1. Processibility and surface appearance

The onset of sharkskin of neat LLDPE film was observed above 30 rpm (mass flow rate of 2.5 kg/h, apparent shear rate of 37.2 s^{-1}). However, the sharkskin of P3GA0.5/LLDPE did not occur even at 50 rpm (mass flow rate 3.5 kg/h, apparent shear rate of 51.3 s^{-1}), the highest extruder speed used in this study. Therefore, the addition of HBP allows a 1.4 times increase (at least) in processing rate without causing surface defects. Also, the sharkskin was eliminated as the hyperbranched polymer came through the die and no preprocessing time was needed. This same observation was made by Hong et al. [24] in their study of fiber spinning.

Fig. 1 clearly demonstrates that the sharkskin was completely eliminated with the addition of 0.5% HBP at the same throughput. However, it was observed that P3GA0.5/LLDPE films were slightly opaque when compared with the neat LLDPE film. Light transmission analysis also shows that the P3GA0.5/LLDPE film has lower light transmission within visible light wavelengths (400–800 nm). The light transmission at a wavelength of 500 nm for pure LLDPE film was 62% while that of the P3GA0.5/LLDPE film was 47%. The results suggest that the HBP and LLDPE did not blend homogeneously and inspection of the film revealed that two layer types appeared to be present which is now justified.

Surface analysis (XPS, discussed below) showed similar results to what Hong et al. [24] found in fiber extrusion, a five times excess of HBP was present at the film surface. Hong et al. showed a central region devoid of HBP was present in a fiber extruded under identical conditions to those here. Near the surface, transmission electron microscopy showed a unique morphology consisting of 50 nm diameter HBP droplets dispersed in LLDPE (denoted as 'emulsion') was present in the fiber. We hypothesize that two separate layer types are present in the film; a central layer devoid of HBP and two surface layers of similar morphology to the fiber surface. We justify this by measuring the same surface excess via XPS as discussed below. The layered morphology may therefore induce the light scattering and consequently cause the opacity or scattering induced by crystallites inherent in the HBP could produce the same effect. Note that the emulsion layer was firmly adhered to the central, bulk LLDPE layer. However, the stability of the emulsion layer is to be established.

3.2. Surface analysis

Fig. 2 shows that gloss of the P3GA0.5/LLDPE film was

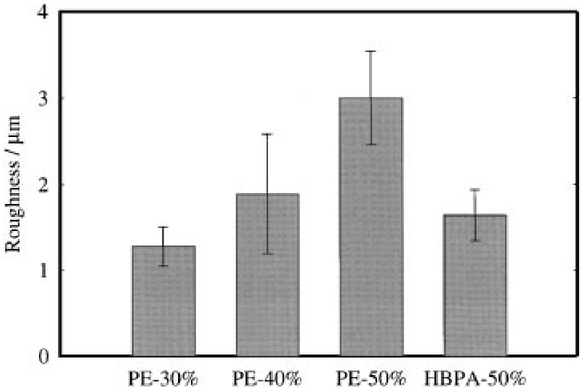

Fig. 3. Comparison of roughness for the neat LLDPE and P3GA0.5/LLDPE blend films manufactured at different extruder speeds expressed as a percentage of full RPM's.

reduced compared with that of the neat LLDPE film. This is in accordance with the results from light transmission analysis discussed above. However, the roughness of P3GA0.5/LLDPE film was improved significantly (Fig. 3) as a consequence of sharkskin elimination which can be beneficial to the film blowing industry. The reason for the loss of gloss and light transmission is probably related to the inherent crystallinity of the HBP used here (discussed below). The native HBP, without the C_{20}–$_{22}$ alkane end groups, is amorphous with a glass transition temperature of approximately 35°C while alkane end groups impart significant crystallinity and melt [56]. This is due to approximately 50% of the macromolecule being end-groups. Of course, this loss of gloss and light transmission may be considered deleterious to the film properties, however, it is our purpose here to demonstrate the principle of rapid, one-shot surface modification and not the production of clear film.

The P3GA0.5/LLDPE film XPS spectrum revealed an oxygen peak at a binding energy of 532.0 eV, and this charge was corrected for the C–C bond to 285.0 eV. There was no trace of oxygen observed in the control sample LLDPE. According to the calculation of atomic concentration on the surface, there was excess oxygen (ca. 5-fold increase of percentage oxygen) attached to carbon on the surface. Hence, the result indicates there was a tendency for HBP to migrate to the surface of the polymer blend when subjected to heating and shear (i.e. during extrusion) or/and during the film formation (i.e. after extrusion).

3.3. Mechanical testing

Table 1 shows there was a slight decrease in tensile strength and on the elongation at break of P3GA0.5/LLDPE films compared with those of neat LLDPE films. There was also an improvement in the 2% secant modulus of P3GA0.5/LLDPE films. However, the change in the mechanical properties is considered minimal, approximately 20% decrease in tensile strength was noted. Film producers are, of course, concerned with any change in

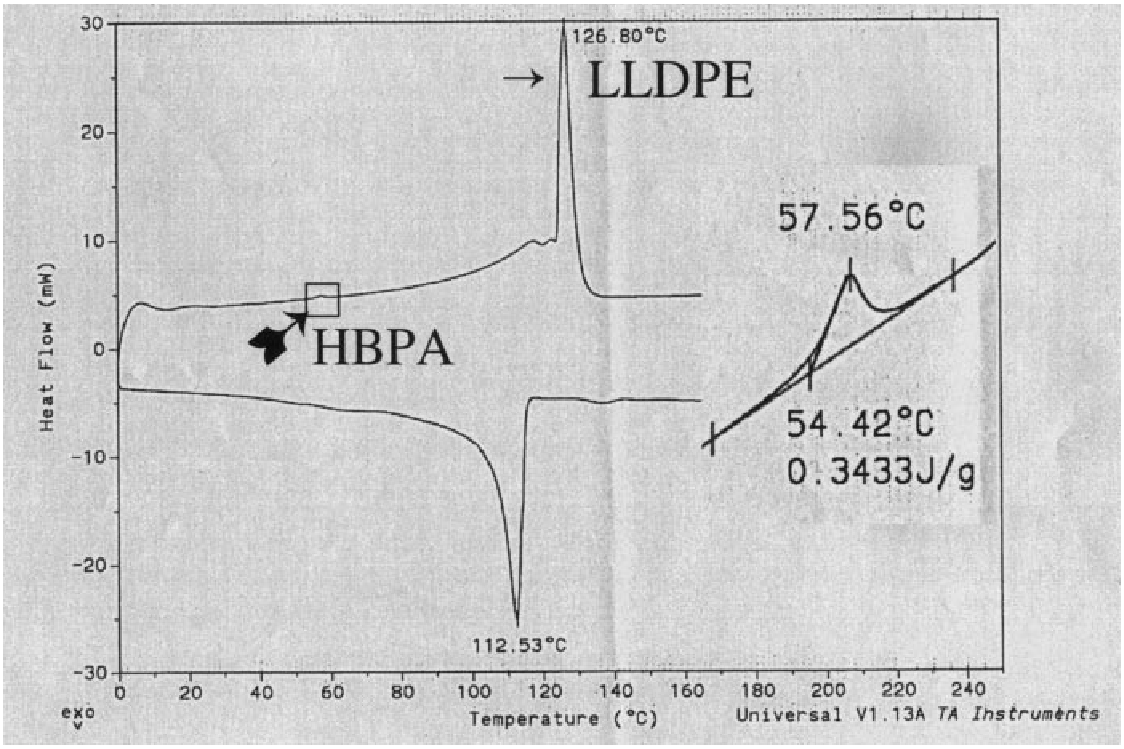

Fig. 4. Differential Scanning Calorimetry scans of LLDPE film and P3GA0.5/LLDPE blend film. The inset shows the DSC scan for the neat hyperbranched polymer. The ratio of the peak area magnitudes shows there is 0.46 wt% hyperbranched polymer in the blend in good agreement with the bulk mixture value of 0.5 wt%.

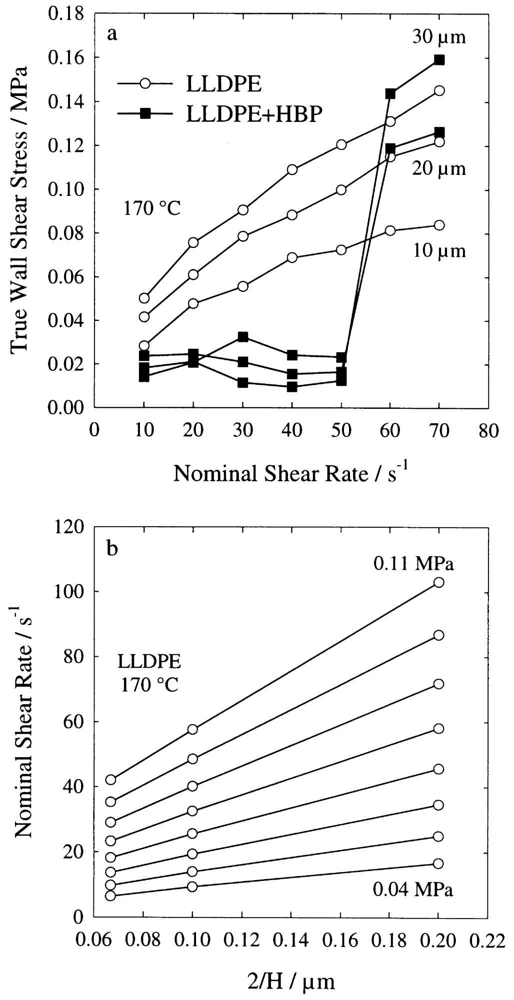

Fig. 5. (a) Plot of true wall shear stress versus nominal shear rate for LLDPE and the HBP blend at various gaps; 10, 20, 30 μm. (b) Plot to determine the slip velocity for pure LLDPE using the data in Fig. 5a. The assumed stress levels were 0.04–0.11 MPa in 0.01 MPa steps.

the mechanical properties and the loss of tensile strength may prohibit usage. The additive we have used here, P3GA, is merely one of many possible HBP additives and optimization of the mechanical properties has not been performed.

3.4. Thermal characterization

The DSC experiments (Fig. 4) showed that the films provide two definite melting points, one associated with the chain end functionalized HBP, and the other with LLDPE. Neither of these transitions have been significantly reduced or increased compared with those recorded for pure LLDPE. We assume this result indicates there are two separate phases in the solid state of the blend. Consequently, we conclude that the HBP used here and LLDPE are immiscible. The conclusion corresponded with the observations mentioned above. Comparing the area of the heat flow melting curves of pure HBP and that of P3GA0.5/LLDPE, the DSC scan suggested the blend contained 0.46% of P3GA which is within the experimental error of the bulk blend composition. Thus, complete phase separation has occurred which concurs with the transmission electron microscopy (TEM) study we performed on extruded fibers in our previous study [24]. The TEM micrographs demonstrated that P3GA phase separated to droplets of order 50 nm in diameter and were present mostly near the fiber surface.

3.5. Slip testing

Samples were prepared similar to our previous study [24] by careful pressing of a fiber to a thin sheet. The pressing was performed under mild pressure and at a temperature slightly above the melting point of LLDPE. We have assumed that this technique did not greatly disturb the native, inhomogeneous structure. Discs were then stamped from the sheet to fit the 7.9 mm diameter parallel plate fixture for rheological testing. This experimental technique provided some intriguing results. Excessive slip was assumed to be present due to the near constant torque values observed, even with increasing shear rate, at each gap tested; this is suspected to be caused by the phase separation of the heterogeneous blend, especially at the metal interface that effectively produces a lubricating layer at both metal surfaces. Fig. 5a shows the true wall shear stress versus nominal shear rate (step 1. in the above data analysis procedure). One can clearly see the stress (or equivalently torque) values were much smaller for the HBP blend than the pure LLDPE indicative again of excessive slip. Note the blend's data points at larger shear rates show the shear stress approaches those for the pure LLDPE, these data were difficult to gather and we do not want to emphasize their importance. They are shown for completeness. The full slip data analysis could not be performed for the blend, however, it could for the pure LLDPE. Fig. 5b shows step 3 in the above slip analysis and the data fall on straight lines for each stress level justifying our experiment analysis. Full data and analysis for a similar LLDPE are presented by Awati et al. [60].

The existence of a 'slip' or emulsion layer between the metal surfaces and the bulk material is supported by the fact there was no observed adhesion of the polymer to either plate since at the end of testing, the bulk disc could be simply peeled off either of the plates. Pure LLDPE was difficult to clean off the plates.

The slip testing results may also offer one of the reasons, from the rheological point of view, why and how the addition of HBP enhances the processing and improves surface appearance. With the framework of our study, the results indicate that wall slippage cannot be held responsible for the surface defects as some other investigators have suggested [41,42]. It is known when polymers are highly entangled, macroscopic slip is observed at the die wall [45]. HBP are not highly entangled melts [61] and may exist as discrete 'globules' [62]. The resultant interactions of HBP with metal surfaces are suggested to be significantly different to those noted for linear polymers. However, we speculate that similar to highly entangled polymers, such ‘globular’ structures are also likely to induce slip, although it may be due to a different mechanism. We have not yet established the mechanism of increased slip, however, we suggest it may be the result from two different scenarios.

The present study suggested that the HBP either forms a discrete phase-separated layer at the wall or the additive was simply more concentrated in a ‘layer’ between the polymer bulk (mixture) and the metal surfaces of the extruder and die. Regardless, the presence of HBP causes a reduced (near-Newtonian) viscosity layer at the surface [24,30,61], therefore, higher shear rates are permitted prior to the onset of surface defects or sharkskin that occur at a constant stress level [36]. Alternatively, molecules with a ‘globular’ structure, which have a lower contacting surface area, may cause a disruption or change in the surface interaction and/or energetics of the bulk melt near the surface, creating less overall adhesion. In other words, such a globular structure may possibly induce the occurrence of slip. Hence slip, very likely, plays a considerable role on eliminating the sharkskin. In part, this conclusion coincides with the interpretation proposed by Cogswell and other investigators.

4. Conclusion

The addition of HBP to LLDPE successfully eliminates surface defects in the normal tubular film blowing process, with no significant changes on overall physical properties. Processibility of the blend is improved significantly through the addition of HBP. The HBP used in this study and LLDPE form an immiscible blend, and importantly the HBP has a tendency to migrate to the surface. It seems to form a lubricating layer of HBP or a HBP-rich mixture on the surface. Therefore, it is possible to produce LLDPE films with high surface activity, which have a potential for surface modification to create desired surface properties according to an end-user’s requirements. Such a layer may induce either a reduction of viscosity or a ‘cohesion’ failure (i.e. slip) at the surface, or both. A rheological study on slip confirms the presence of extensive slip under shear, which may in part contribute to the sharkskin elimination.

Acknowledgements

The authors are grateful to Dr Tri Le and Mr Barrie Wood at the University of Queensland for their assistance in the surface analysis. The help of Mr. Mark Coghill (RioTinto) in performing the gloss and surface roughness tests is also gratefully acknowledged. Discussions with Dr Peter Halley were greatly appreciated. This work is partially supported by The University of Queensland Postdoctoral Fellowship Scheme (Australia), the Early Career Researcher Grants Scheme (Australia), and by the NSF Center for Polymeric Interfaces and Macromolecular Assemblies (USA).

References

[1] Briston JH. Plastics films. 3rd ed., London: Longman, 1988.
[2] Ramamurthy AV. J Rheol 1986;30:337.
[3] La Mantia FP, Geraci C, Vinci M, Pedretti U, Roggero A, Minkova LI, Magagnini PL. J Appl Polym Sci 1995;58:911.
[4] Lichkus AM, Harrison IR. SPE ANTEC ’92, 1992. p. 2257.
[5] La Mantia FP, editor. Thermotropic liquid crystal polymer blends Lancaster: Technomic, 1993.
[6] Harada T, Tomari K, Hamamoto A, Tonogai S, Sakaura K, Nagai S, Yamaoka K. SPE Antec ’2, 1992. p. 376.
[7] Hsu TC, Lichkus AM, Harrison IR. Polym Engng Sci 1993;33:860.
[8] Fraser WA, Herdle WB. RETEC Polyolefin V. Fifth international conference on polyolefins, Houston, 1987. p. 301.
[9] Schumacher PA. J Plast Film Sheet 1987;3:118.
[10] Schumacher P. SPI/SPE ’86, Atlanta, 1986. p. 78.
[11] Rudin A, Blacklock JE, Nam S, Worm AT. ANTEC ’86, 1986. p. 1154.
[12] Blong TJ, Duchesne D. Plastics Compounding 1990;13:50.
[13] Callaghan M. Plastics Technol. July 1987:61.
[14] Johnson BV, Blong TJ, Schreiber HP. Fourth International Polymer Processing Society Meeting, Orlando, 1988. p. 17.
[15] De Smedt C, Nam S. Plast Rubber Process Appl 1987;8:11.
[16] Rudin A, Worm AT, Blacklock JE. Processing and property enhancement utilizing modifiers and additives in polymers. First International conference. Newark, 1985.
[17] Klein DF. RETEC Polyolefins V. Fifth international conference on polyolefins, Houston, 1987. p. 285.
[18] Rudin A, Worm AT, Blacklock JE. J Plast Film Sheet 1985;1:189.
[19] Johnson BV, Kunde JM. Plast Engng 1988;44:43.
[20] Stewart CW, Dealy JM. J Rheol 1992;36:967.
[21] Hatzikiriakos SG, Stewart CW, Dealy JM. Int Polym Process 1993;8:30.
[22] Hatzikiriakos SG, Dealy JM. Int Polym Process 1993;8:36.
[23] Stewart CW, McMinn RS, Stika KM. J Reinforced Plast Composites 1993;12:633.
[24] Hong Y, Cooper-White JJ, Mackay ME, Hawker CJ, Malmström E, Rehnberg N. J Rheol 1999;43:781.
[25] Dvornic PR, Tomalia DA. Curr Opin Coll Interf Sci 1996;1:221.
[26] Frey H, Lach C, Lorenz K. Adv Mater 1998;10:279.
[27] Hawker CJ, Fréchet JMJ. J Am Chem Soc 1990;112:7638.
[28] Kim YH. Macromolecular design of polymeric materials, vol. 40 1997 (p. 365).
[29] Hobson LJ, Harrison RM. Curr Opin Solid State Mater Sci 1997;2:683.
[30] Farrington PJ, Hawker CJ, Fréchet JMJ, Mackay ME. Macromolecules 1998;31:5043.
[31] Fréchet JMJ, Hawker CJ, Gitsov I, Leon JW. J Macromol Sci Pure Appl Chem 1996;33:1399.
[32] Fréchet JMJ. Science 1994;263:1710.
[33] Kim YH, Webster OW. Macromolecules 1992;25:5561.
[34] Tordella JP. In: Eirich FR, editor. Rheology, 5. New York: Academic Press, 1969.
[35] White JL. Appl Polym Symp 1973;20:155.
[36] Petrie CJS, Denn MM. AIChE J 1976;22:209.
[37] Ballenger TF, Chen I-J, Crowder JW, Hagler GE, Bogue DC, White JL. Trans Soc Rheol 1971;15:195.
[38] Denn MM. Annu Rev Fluid Mech 1990;22:13.
[39] Denn MM. Chem Engng Ed 1994;Summer:163.
[40] Piau JM, Kissi NE, Toussaint F, Mezghani A. Rheol Acta 1995;34:40.
[41] Benbow JJ, Charley RV, Lamb P. Nature 1961;192:223.
[42] Benbow JJ, Lamb P. Soc Petrol Engng Trans 1962;3:7.

[43] Kalika DS, Denn MM. J Rheol 1987;31:815.
[44] Hill DA, Hasegawa T, Denn MM. J Rheol 1990;34:891.
[45] ElKissi N, Piau JM. J Non-Newtonian Fluid Mech 1990;37:55.
[46] McLeish TCB. J Polym Sci 1987;B25:2253.
[47] Weil A. J Non-Newtonian Fluid Mech 1980;7:303.
[48] den Otter JL. Plast Polym 1970;38:155.
[49] Piau JM, ElKissi N, Tremblay B. J Non-Newtonian Fluid Mech 1990;34:145.
[50] Cogswell FN. J Non-Newtonian Fluid Mech 1977;2:37.
[51] Sornberger G, Quantin JC, Fajolle R, Vergnes B, Agassant JF. J Non-Newtonian Fluid Mech 1987;23:123.
[52] Tremblay B. J Rheol 1991;35:985.
[53] Howells ER, Benbow JJ. Trans Plast Inst 1962;30:240.
[54] Kurtz SJ. In: Mena B, Garcia-Rejón A, Nafaile CR, editors. Advances in rheology, Mexico: Univerisdad Nacional Autonoma de Mexico, 1984. p. 197.
[55] Kurtz SJ. In: Moldenaers P, Keunings R, editors. Theroretical and applied rheology—Proceedings of the XI Congress on Rheology, Belgium, Amsterdam: Elsevier, 1992. p. 377.
[56] Malmström E, Johanson M, Hult A. Macromol Chem Phys 1996;197:3199.
[57] Ward RJ, Wood BJ. Surf Interf Anal 1992;18:679.
[58] Mackay ME, Henson DJ. J Rheol 1998;42:1505.
[59] Yoshimura A, Prud'homme RK. J Rheol 1988;32:53.
[60] Awati KM, Park Y, Weisser E, Mackay ME. J Non-Newtonian Fluid Mech 2000 (in press).
[61] Hawker CJ, Farrington PJ, Mackay ME, Wooley KL, Fréchet JMJ. J Am Chem Soc 1995;117:4409.
[62] Dagani R. Chemical and Engineering News, June 1996.
[63] Gorman C. Adv Mater 1998;10:295.
[64] Fisher M, Vogtle F. Angew Chem Int Ed Engl 1999;38:885.
[65] Webster OW. Science 1994;251:887.
[66] Fréchet JMJ. Science 1994;263:1710.